A NEW MODEL FOR THE TOPOLOGY OF MAGNETIC CLOUDS IN THE SOLAR WIND

M. A. HIDALGO[1], C. CID[1], J. MEDINA[1] and A. F. VIÑAS[2]
[1]*Departamento de Física, Universidad de Alcalá, Alcalá de Henares, Madrid, Spain*
(E-mail: hidalgo@grc.fis.alcala.es)
[2]*NASA Goddard Space Flight Center, Laboratory for Extraterrestrial Physics, Greenbelt, MD 20771, U.S.A.*

(Received 18 May 1999; accepted 22 December 1999)

Abstract. We present a model that describes the topology of a magnetic cloud. The model relates the magnetic field vector and current density of the cloud without assuming the force-free condition. Fitting the model to the experimental data we obtain the current density, the attitude of the axis and the relative closest-approach distance between the spacecraft and the cloud axis. In this paper, several magnetic clouds of 1997 are analyzed. The results indicate that the topology presented in this paper explains the magnetic field inside a MC better than force-free models. A current density of the order of 10^{-12} C m^{-2} s^{-1} is obtained in the fitting of all the events.

1. Introduction

Burlaga *et al.* (1981) introduced the term magnetic cloud (MC) for a structure in the solar wind that follows an interplanetary shock and shows a smooth rotation of the magnetic field. Other features of these events are low proton β and low proton temperature and a relatively high magnetic field strength. Nowadays, the analysis of spacecraft data reveals that these events are common in the solar wind (e.g., Klein and Burlaga, 1982; Bothmer and Schwenn, 1998) and are considered a subset of interplanetary ejecta or coronal mass ejections (CMEs) in the solar wind. These events are not always associated with interplanetary shocks but only when they travel faster than the ambient solar wind. In such cases shocks serve as useful fiducials for identifying fast CMEs in the solar wind (e.g., Richardson and Cane, 1993). Plasma and field signatures of CMEs have been recognized in the solar wind a number of hours after shock passage. Most of these anomalous signatures are also observed in absence of shocks, where they serve to identify low-speed CMEs (Gosling, 1993). Counter-streaming fluxes of suprathermal solar wind halo electrons with energies above 80 eV and bidirectional energetic ions flows (above 0.8 MeV) are also useful to identify CMEs in the solar wind (Richardson and Reames, 1993). This signature is related to the characteristic closed magnetic field topology of CMEs, different from the open magnetic topology of the normal solar wind. Besides the identification of MCs, locating cloud boundaries is an open problem (Lepping, Jones, and Burlaga, 1990). Crooker, Gosling, and Kahler (1998)

Solar Physics **194:** 165–174, 2000.

compared cloud boundaries with the boundaries of counter-streaming electrons for 14 clouds identified by Zhang and Burlaga (1988). They showed that those clouds are usually spatially shorter than the interval defined by counter-streaming electrons, suggesting that the clouds are parts of larger transient structures. Recent studies (Osherovich *et al.*, 1993) have identified the cloud boundaries in terms of changes of the thermodynamic properties of the plasma. This study has shown a deviation of the thermodynamic behavior of protons in the region near the boundaries of MCs compared with those that surround the cloud itself.

Goldstein (1983) proposed the idea that a MC can be explained by twisted flux rope with force-free configuration, described by $\nabla \times \mathbf{B} = \alpha(\mathbf{r})\mathbf{B}$. Marusbashi (1986) first proved this idea with data using a simple force-free model. Restricting attention to the case where the parameter α is independent of position several solutions have been obtained. Lundquist (1950) showed static axially symmetric fields solution of this equation in cylindrical geometry. This solution depends on the zeroth- and first-order Bessel functions. Lepping, Jones, and Burlaga (1990) developed a least-squares fitting algorithm based on this model. A different treatment is that of Chen (1996) where the flux rope is already formed near the Sun and moves to the interplanetary medium. The field is due only to the current inside the loop and it need not be force-free.

This paper presents a simple model to analyze MCs in the solar wind using the magnetic field vector obtained from spacecraft observations. The model does not assume the force-free condition. A detailed description of the model is given in Section 2. In Section 3, we report the results of the fitting of the model to the experimental data. We summarize and discuss the results in the last section.

2. Model Description

In this paper we assume that a MC may be represented as a flux rope (see the review by Burlaga, 1991) although it need not be force-free. Thus, it seems convenient to describe it with a toroidal reference system where the minor axis of the torus coincides with the axis of the MC. In this frame of reference the magnetic field lines have only two components: one along the cloud axis and the other one around it. That is, the magnetic field can be decomposed into a toroidal (B_{ψ}^{MC}) component and a poloidal (B_{φ}^{MC}) one. For the topology of the flux rope that we have assumed there is no radial component.

In our description the MC topology is modeled by analyzing separately the toroidal and poloidal components of the magnetic field, and relating them to the poloidal and toroidal components of the current density, respectively.

We assume that the poloidal component of the magnetic field is a consequence of the toroidal component of the current density. Then, supposing that the flux rope cross-section has a circular shape and that in this section the toroidal component

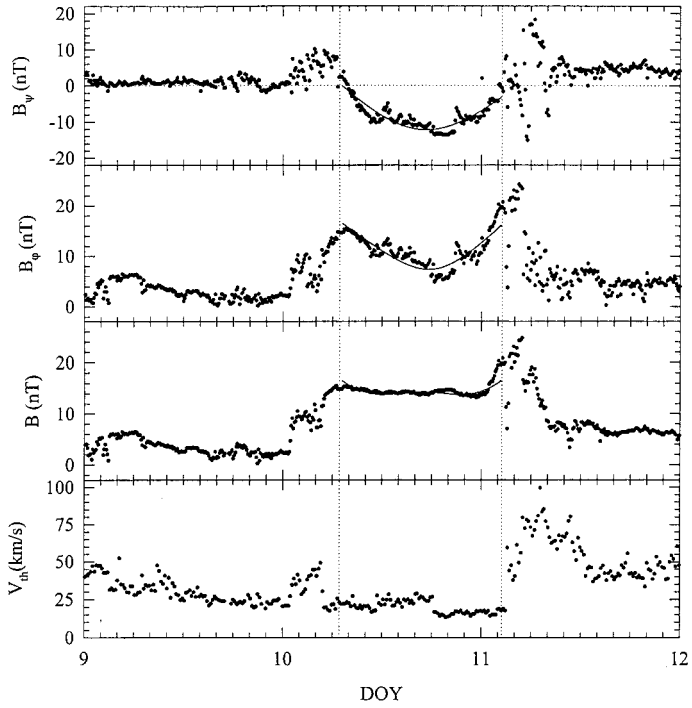

Figure 1. Magnetic field strength, toroidal and poloidal components of the magnetic field (B_ψ, B_φ, B) together with thermal velocity (V_{th}) surrounding the 10 January 1997 event observed by WIND. Dots represent the experimental data. The solid lines are the fitted components of our modeled magnetic cloud structure. The vertical dot lines represent the start and end time of the cloud.

of the current distribution is uniform, the poloidal component of the magnetic field inside the cloud can be written as

$$B_\varphi^{MC} = \frac{\mu_0}{2} j_\psi r \ , \tag{1}$$

where μ_0 is the vacuum permeability, r the distance to the cloud axis (or minor radius) and j_ψ the toroidal component of the current density.

Similarly, we suppose that the toroidal magnetic field component is due to the poloidal component of the current density. Assuming that the MC is locally axial symmetric and the poloidal current distribution is uniform, the expression

$$B_\psi^{MC} = \frac{\mu_0}{2} j_\varphi \frac{(\rho_0 - r)^2 - (\rho_0 - R)^2}{(\rho_0 - r)} \tag{2}$$

can be used for the toroidal component of the magnetic field. R is the radius of the MC (or maximum minor radius of the cloud) and ρ_0 the distance from the cloud axis to the center of the torus (or the major radius of the minor axis).

When the cloud is observed in the solar wind, the axis makes an angle θ (latitude) with respect to the ecliptic plane, it has a longitude, ϕ, in the ecliptic plane,

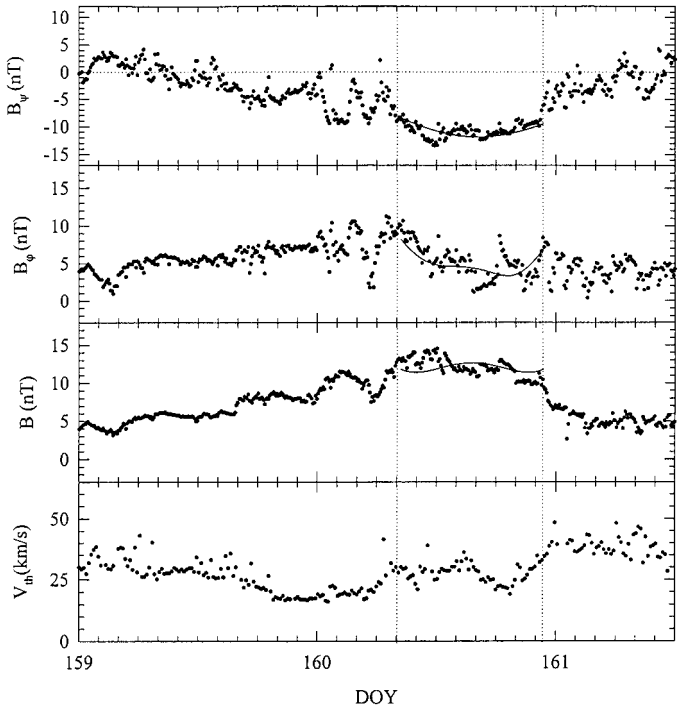

Figure 2. Magnetic field strength, toroidal and poloidal components of the magnetic field (B_ψ, B_φ, B) together with thermal velocity (V_{th}) surrounding the 8 June 1997 event observed by WIND. Dots represent the experimental data. The solid lines are the fitted components of our modeled magnetic cloud structure. The vertical dot lines represent the start and end time of the cloud.

and the spacecraft does not pass through the cloud axis. In this scenario, we have to transform the expressions for the cloud magnetic field components, Equations (1) and (2), to the GSE coordinate system (which experimental data are refered to) taking into account the attitude of the cloud axis and the spacecraft path. After this transformation we obtain expressions for the theoretical magnetic field components in the GSE system depending on θ, ϕ and y_0.

Because the large value of the x-GSE component of the solar wind velocity in the MC intervals, the path of the spacecraft relative to the cloud is almost parallel to the x-GSE direction. We establish the origin of the experimental coordinate system at the encounter of the spacecraft with the cloud (at $t = t_0$) and the axis-directions are those of the GSE system. For any other time, t, we calculate the corresponding position (x, 0, 0) using the expression $x = v_{sw}(t - t_0)$, until the spacecraft leaves the cloud at $t = t_1$.

We transform the measurements of the spacecraft made in the GSE frame reference (B_x^{GSE}, B_y^{GSE}, B_z^{GSE}), through the expressions

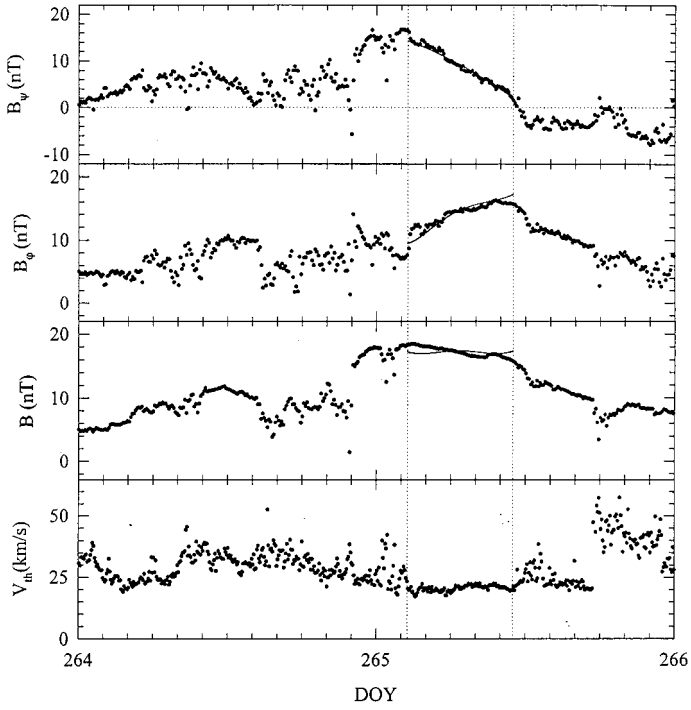

Figure 3. Magnetic field strength, toroidal and poloidal components of the magnetic field (B_ψ, B_φ, B) together with thermal velocity (V_{th}) surrounding the 21 September 1997 event observed by WIND. Dots represent the experimental data. The solid lines are the fitted components of our modeled magnetic cloud structure. The vertical dot lines represent the start and end time of the cloud.

$$\begin{aligned} B_\varphi^{\exp} &= \sqrt{(B_x^{\mathrm{GSE}})^2 + (B_z^{\mathrm{GSE}})^2}\,, \\ B_\psi^{\exp} &= B_y^{\mathrm{GSE}}\,, \\ B_r^{\exp} &= 0\,. \end{aligned} \tag{3}$$

If the flux rope has its major axis parallel to the z-GSE, its minor axis lying on the xy-GSE plane and the spacecraft path in the x-axis, the components $B_\psi^{\exp}$ and $B_\varphi^{\exp}$ would agree with the magnetic field in the cloud reference system, B_ψ^{MC} and B_φ^{MC}. However, in a real case, we need to relate the components (B_ψ^{MC}, B_φ^{MC}) with ($B_\psi^{\exp}$, $B_\varphi^{\exp}$) through θ, ϕ and y_0, as we explained above.

Our set of data consists of a magnetic vector data ($B_\psi^{\exp}$, $B_\varphi^{\exp}$) for every position along the spacecraft path (x, 0, 0). Fitting the model to these data, we can obtain the five free parameters: the current density components, j_ψ and j_φ, the attitude of the axis θ, ϕ and the relative closest-approach distance, y_0. Note that the radius of the cloud, R, in Equation (2) can also be expressed as a function of the parameters θ, ϕ, and y_0, and the time values of the boundaries, t_0 and t_1. We apply a least-squares

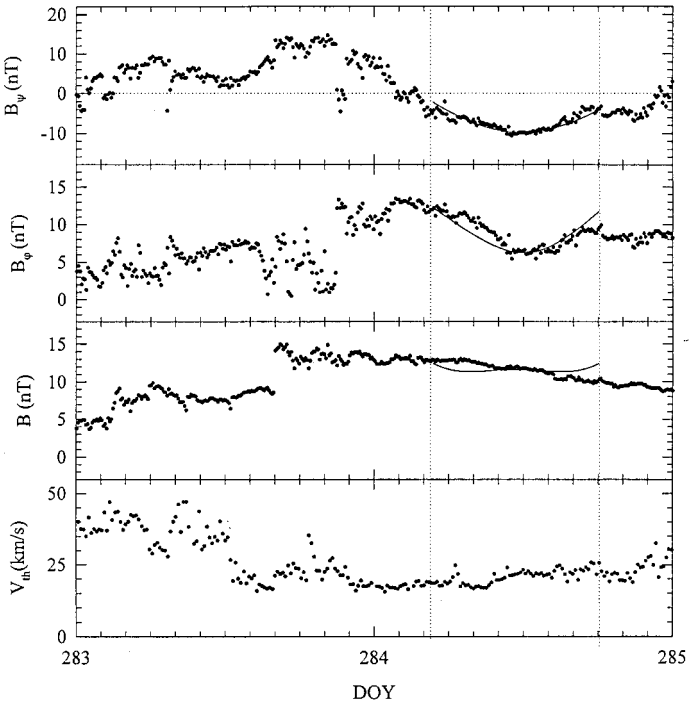

Figure 4. Magnetic field strength, toroidal and poloidal components of the magnetic field (B_ψ, B_φ, B) together with thermal velocity (V_{th}) surrounding the 10 October 1997 event observed by WIND. Dots represent the experimental data. The solid lines are the fitted components of our modeled magnetic cloud structure. The vertical dot lines represent the start and end time of the cloud.

program that uses the Marquardt algorithm (Marquardt, 1963) which minimized the χ^2:

$$\chi^2 = \sum [(B_\varphi^{\exp} - B_\varphi^{\mathrm{mod}})^2 + (B_\psi^{\exp} - B_\psi^{\mathrm{mod}})^2]/N \ , \tag{4}$$

where the indexes exp and mod are referred to the experimental and model data, respectively, and N is the number of field vectors. It is understood that $B^{\exp}$ and B^{mod} are unit normalized; therefore χ^2 is dimensionless.

3. Observations

For this paper we have selected five magnetic clouds identified in WIND magnetic field and plasma data. These candidates are provided by WIND-MFI's Website under the URL *http://lepmfi.gsfc.nasa.gov/mfi/mag_cloud_pub1.html\#table.* The period covered is the year 1997, and the study is based in five better (those of quality 1), out of thirteen candidates. One of these clouds has been recently analyzed with a force-free model (Burlaga *et al.*, 1998).

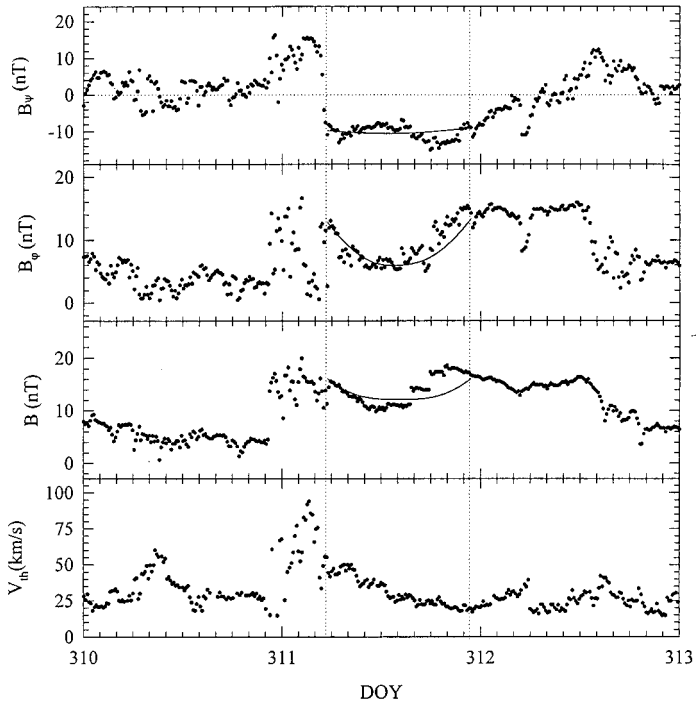

Figure 5. Magnetic field strength, toroidal and poloidal components of the magnetic field (B_ψ, B_φ, B) together with thermal velocity (V_{th}) surrounding the 7 November 1997 event observed by WIND. Dots represent the experimental data. The solid lines are the fitted components of our modeled magnetic cloud structure. The vertical dot lines represent the start and end time of the cloud.

Following the well-established definition of MC (Burlaga, 1981), we select the interval that presents the lowest thermal velocity as the MC interval. Although sometimes the boundaries selected do not coincide with those provided in the web-page, we want to be consistent with the definition of MC. Once we have determined the values of t_0 and t_1, we obtain the mean solar wind velocity measured inside the cloud, V_{SW}. Having this value into account, the measured magnetic field at different stages of observation can be related to different positions inside the cloud, as we explained above.

In order to continue the fit, we have made hourly averages of the magnetic field data. Besides, as a first approach, we take the distance from the cloud axis to the center of the torus, ρ_0, to be 0.5 AU. Figure 1 shows magnetic field data and the thermal velocity around a magnetic cloud occurring on day 10 of 1997. The cloud's assumed start and end times are marked by vertical dotted lines on the figure. These times are listed in Table I and are in agreement both with the lowest thermal velocity interval and with that interval selected by Burlaga *et al.* (1998). We summarize in the table the parameters obtained from the fitting of the model to the experimental data. Notice that the latitude of the cloud axis ($\theta = 6°$) and

TABLE I

Parameters for every MC studied: Start and end time, obtained with a precision of half an hour (columns 2 and 3). Column 4 is the mean solar wind velocity for the interval of the MC and column 5 is the radius of the cloud estimated with the model. Finally, it also gives the parameters obtained from the fitting of the model to the five MCs analyzed in this paper. The fitting parameters are the toroidal and poloidal components of the current density (columns 6–7), the latitude (column 8), longitude (column 9) of the cloud axis, and the closest-approach distance (column 10). In the last column the χ^2 values obtained are detailed.

Event (Year-month)	Start (Doy-hour)	End (Doy-hour)	V_{sw} (km s^{-1})	R (10^9 m)	j_ψ (10^{-12} C m^{-2} s^{-1})	j_φ (10^{-12} C m^{-2} s^{-1})	θ (deg)	ϕ (deg)	y_0/R	χ^2
97-01	10-07	11-02	438	17.9	1.46	1.17	6	259	0.57	0.029
97-06	160-08	160-23	373	6.11	3.06	5.91	2	200	0.82	0.024
97-09	265-02	265-11	411	3.76	7.35	16.3	12	172	0.90	0.002
97-10	284-05	284-18	396	13.4	1.48	1.66	6	251	0.74	0.011
97-11	311-05	312-02	435	1.79	14.3	8.19	−0.3	189	0.59	0.025

the longitude ($\phi = 259°$) are the same as those obtained from a force-free model (see Burlaga *et al.*, 1998). The value of the minimum approach distance is the main difference between the two models. In the case of our model, $y_0/R = 0.57$, that is four times the value obtained with the other model. Maybe this could explain why the variation of the magnetic field strength is modeled more accurately with our model.

Figures 2–5 show the model predictions (solid lines) superimposed on the experimental data (dots) for the other four events analyzed. Notice that the model fits very well not only for B_ψ and B_φ, but also for B.

The event of September (Figure 3) should be considered with special attention. First of all, the boundaries that we have established for the cloud (see Table I) are not the same as those from the web-page (from doy 264 at 22 hr to doy 265 at 23 hr). We have selected those boundaries using the lowest thermal velocity interval. Anyway, although we think that the other boundaries are not consistent with that definition, we have tried to fit the magnetic field in that interval but we cannot obtain a proper fit. As Figure 3 shows, our model accurately reproduces the magnetic field measured although the magnetic field components do not change sign.

4. Summary and Discussion

We have presented a model for the topology of a MC which relates the magnetic field with the current density of the cloud. The model is not based on a force-free field configuration. Although we consider a flux rope, we make the assumption of a locally cylindrically symmetric configuration. The mathematical expressions for the magnetic field, Equations (1) and (2), are simpler than those deduced from force-free models. After a transformation to change the reference system, we obtain the equations used in the fitting procedure.

The five-parameter fit provides the latitude and longitude of the cloud axis, the closest-approach distance, and the current density components, j_ψ and j_φ. In all cases analyzed, the current density inside the cloud is of the order of 10^{-12} C m^{-2} s^{-1}. The quality of the results is based on computation of χ^2. The value obtained for the 10 January 1997 event (see Table I) is less than that obtained with a force-free model. We want to remark that our model fits both the direction of the magnetic field vector and its magnitude. As shown in the Figures 1–5, the model reproduces the magnetic field data accurately.

It is our intention for future work to generalize the model to include elliptic cross-sections and non-uniform current densities.

Acknowledgements

The authors thank K. Ogilvie, R. Fitzenreiter, and R. Lepping (Goddard Space Flight Center, Greenbelt, MD, USA) for permission to use the WIND data.

References

Bothmer, V. and Schwenn, R.: 1998, *Ann. Geophys.* **16**, 1.
Burlaga, L. F.: 1991, in R. Schwenn and E. Marsch (eds.), *Physics of the Inner Heliosphere II*, Springer-Verlag, Berlin, p. 1.
Burlaga, L. F. , Sittler, E., Mariani, F., and Schwenn, R.: 1981, *J. Geophys. Res.* **86**, 6673.
Burlaga, L. *et al*.: 1998, *J. Geophys. Res.* **103**, 277.
Chen, J.: 1996, *J. Geophys. Res.* **101**, 27 499.
Crooker, N. U., Gosling, J. T., and Kahler, S. W.: 1998, *J. Geophys. Res.* **103**, 301.
Goldstein, H.: 1983, *NASA Conf. Publ.*, CP-2280, 731.
Gosling J. T.: 1993, *J. Geophys. Res.* **98**, 18 937.
Klein, L. W. and Burlaga, L. F.: 1982, *J. Geophys. Res.* **87**, 613.
Lepping, R. P., Jones, J. A., and Burlaga, L. F.: 1990, *J. Geophys. Res.* **95**, 11 957.
Lundquist, S.: 1950, *Ark. Fys.* **2**, 361.
Marquardt, D. W.: 1963, *J. Soc. Ind. Appl. Math.*, **11**, 431.
Marubashi, K.: 1986, *Adv. Space Res.* **6**, 335.
Osherovich, V. A., Farrugia, C. J., Burlaga, L. F., Lepping, R. P., Fainberg, J., and Stone, R. G.. 1993, *J. Geophys. Res.* **98**, 15 331.
Richardson, I. G. and Cane, H. V.: 1993, *J. Geophys. Res.* **98**, 15 295.
Richardson, I. G. and Reames, D. V.: 1993, *Astrophys. J. Suppl. Ser.* **85**, 411.
Zhang, G. and Burlaga, L. F.:1988, *J. Geophys. Res.* **93**, 2511.